НАЦИОНАЛЬНЫЙ ИССЛЕДОВАТЕЛЬСКИЙ
УНИВЕРСИТЕТ

"Transparent" Boundary Conditions

for the Rod Transverse Vibrations Equation

V.A.Gordin and A.A.Shemendyuk

National Research University
Higher School of Economics
Hydrometeorological Center of Russia

November 22, 2018

Introduction

Условие прозрачности границы для выходящих из расчетной области волн = совпадению решения смешанной краевой задачи с такими граничными условиями и с начальными условиями, продолженными нулем на все пространство.
Цель доклада построить их для разностного уравнения, но сначала несколько примеров для дифференциальных.
Рассмотрим уравнение струны $\partial_t^2 u = c^2 \partial_x^2$. Граничные условия $\partial_t u = \pm c \partial_x$ на краях отрезка $[-L/2, L/2]$ иммитируют задачу Коши.
Обычно такие граничные условия ИЗК нелокальны.
Стандартная форма такого условия содержит свертку:

$$\partial_n u = K * u,$$

по времени и касательным к границе переменным.

Introduction

Для волнового уравнения в нечетномерном пространстве, где $n = 2m + 1$ ядро задается формулой

$$K(t, \vec{y}) = \frac{c}{(4\pi)^m \Gamma(m + 1/2)} \left(c^{-2}\partial_t^2 - \Delta'\right)^{m+1} \left[\frac{\chi(ct - |\vec{y}|)}{\sqrt{t^2 - c^{-2}|\vec{y}|}} \right],$$

где Δ' — оператор Лапласа по переменным $\vec{y}$, касательным к границе, Γ — Гамма-функция Эйлера.
Интегрирование в свертке по времени и пространству ведется не везде, а только по обратному световому конусу $|\vec{y} - \vec{z}| \leq (t - s)$.

В четномерном пространстве формула для ядра внешне похожа, но в нечетномерном пространстве можно интегрированием по частям перейти к интегрированию в свертке лишь по границе обратного светового конуса, а в четномерном случае нельзя. Это явление называется лакуной и исследуется в теории Герглотца – Петровского.

Аналогичные ядра получаются для уравнений диффузии, Шрёдингера, но там обратный световой конус не воникает. Интегрировать в свертке надо по всем $\vec{z} \in \mathbb{R}^{n-1}$.

Introduction

The equation of transverse vibrations of a rod (beam) with a circular cross section

$$\rho \frac{\partial^2 u}{\partial t^2} - \frac{\partial}{\partial x}\left[R^2 \rho \frac{\partial^3 u}{\partial x\, \partial t^2}\right] + \frac{\partial^2}{\partial x^2}\left[E R^2 \frac{\partial^2 u}{\partial x^2}\right] = f \qquad (1)$$

has many applications. Here ρ is the density of the rod, R is the radius of the cross section of the rod, E is the Young's modulus of the rod, $u = u(t, x)$ is the transverse displacement of the rod, $x \in [-L/2, L/2]$, L is the length of the rod. The right hand side (forsing) f describes external force.
Eq. (1) is supplemented by two initial conditions:

$$u(0, x) = U_0(x), \quad \partial_t u(0, x) = U_1(x),$$

Crank–Nicolson Approximation

Let us consider Eq. (1) with constant coefficients and with zeroth forcing f:

$$\rho \frac{\partial^2 u}{\partial t^2} - R^2 \rho \frac{\partial^4 u}{\partial^2 t \, \partial^2 x} + ER^2 \frac{\partial^4 u}{\partial^4 x} = 0, \tag{2}$$

and the implicit finite-difference scheme on the five-point stencil of the Crank – Nicolson type that approximates Eq. (2) on the uniform grid with the steps τ with respect to time t and h with respect to spatial variable x:

$$\sigma \left(u_{2h}^{n+1} + u_{-2h}^{n+1} + u_{2h}^{n-1} + u_{-2h}^{n-1} \right) + \beta \left(u_{h}^{n+1} + u_{-h}^{n+1} + u_{h}^{n-1} + u_{-h}^{n-1} \right) +$$
$$+ \alpha \left(u_0^{n+1} + u_0^{n-1} \right) + \gamma \left(u_{-h}^{n} + u_h^n \right) + \delta u_n^n = 0,$$
$$u(0, x_i) = u_0(x_i), \quad u(\tau, x_i) = u_\tau(x_i), \quad i = 0, \ldots, N, \tag{3}$$

Let $\nu = ER^2 \rho^{-1} \cdot \tau^2 h^{-4}$, $\mu = R^2 \cdot h^{-2}$ and $\alpha = 1 + 3\nu + 2\mu$, $\beta = -2\nu - \mu$, $\gamma = 2\mu$, $\delta = -2 - 4\mu$, $\sigma = \nu/2$.

ICP Boundary Condition Construction Algorithm

1. Apply the $\mathcal{Z}$-transformation (discrete analogue of the Laplace integral transformation) in time to Eq. (3) and obtain a linear ordinary finite-difference equation with respect to the variable m; the equation depending on the parameter $z \in \mathbb{C}$.
2. Construct for the corresponding homogeneous finite-difference 4-th order equation a fundamental set of solutions $\{Y_j(m)\}_{j=1}^{4}$, such that solutions $Y_1,\ Y_2$ decrease as $m \to +\infty$, and solutions $Y_3,\ Y_4$ decrease as $m \to -\infty$.
3. Decompose for the right segment's end the obtained growing (as $m \to +\infty$) solutions (functions from the dual variable z with respect to time t) into a series in a neighbourhood of $z = \infty$. For the left end — as $m \to -\infty$.
4. Apply the inverse $\mathcal{Z}$-transformation to the obtained coefficients of the ICP boundary conditions. Introduce the change of variable $\omega = 1/z$ and decompose the symbol into a Taylor series

After $\mathcal{Z}$-transformation of Eq. (3), we get characteristic homogeneous equation

$$\sigma\left(1+\omega^2\right)\left[\lambda+\lambda^{-1}\right]^2+\left(\beta\left(1+\omega^2\right)+\gamma\omega\right)\left[\lambda+\lambda^{-1}\right]+ \\ +\delta\omega+(\alpha-2\sigma)\left(1+\omega^2\right)=0. \tag{4}$$

Substitute variable $\eta=\lambda+\lambda^{-1}$ in Eq. (4) and get

$$\sigma\left(1+\omega^2\right)\eta^2+\left(\beta\left(1+\omega^2\right)+\gamma\omega\right)\eta+\delta\omega+(\alpha-2\sigma)\left(1+\omega^2\right)=0. \tag{5}$$

Roots of Eq. (5) are

$$\eta_{1,2}(\omega)=\frac{-\beta\left(1+\omega^2\right)-\gamma\omega}{2\sigma\left(1+\omega\right)}\mp \\ \mp\frac{\sqrt[+]{\left(\beta\left(1+\omega^2\right)+\gamma\omega\right)^2-4\sigma\left(1+\omega^2\right)\left[\delta\omega+(\alpha-2\sigma)\left(1+\omega^2\right)\right]}}{2\sigma\left(1+\omega\right)}, \tag{6}$$

Construction of ICP

We develop function (6) in the Taylor series at $\omega = 0$:

$$\eta_{1,2}(\omega) = \frac{1}{\nu}\sum_{k=0}^{\infty}(-1)^k\omega^{2k}[(\mu+2\nu)\left(1+\omega^2\right) - 2\mu\omega \mp$$

$$\mp\sqrt{\mu^2-2\nu}\,(1-\omega)\left(\omega^2 - 2\frac{\mu^2}{\mu^2-2\nu}\omega + 1\right)\sum_{n=0}^{\infty}\mathrm{P}_n\left(\frac{\mu^2}{\mu^2-2\nu}\right)\omega^n], \tag{7}$$

where P_n is a Legendre polynomial of degree n. Note that as $\omega \to 0$

$$\eta_j(\omega) = \vartheta_j + r_j(\omega), \tag{8}$$

where $r_j(\omega) \to 0$, $j = 1,\ 2$, and

$$\vartheta_j = \frac{1}{2\sigma}\left[\beta \mp \sqrt{\beta^2 - 4\sigma(\alpha - 2\sigma)}\right] = 2 + \frac{\mu}{\nu} \mp \frac{1}{\nu}\sqrt{\mu^2-2\nu}. \tag{9}$$

Construction of ICP

Let us resolve the relation $\eta = \lambda + \lambda^{-1}$ as a quadratic equation

$$\lambda^2 - \eta\lambda + 1 = 0. \tag{10}$$

For both η_1, η_2 we obtain the following roots of characteristic Eq. (4):

$$\lambda_1 = \frac{\eta_1(\omega)}{2} - \sqrt{\frac{\eta_1^2(\omega)}{4} - 1}, \quad \lambda_2 = \frac{\eta_2(\omega)}{2} - \sqrt{\frac{\eta_2^2(\omega)}{4} - 1},$$
$$\lambda_3 = \frac{\eta_1(\omega)}{2} + \sqrt{\frac{\eta_1^2(\omega)}{4} - 1}, \quad \lambda_4 = \frac{\eta_2(\omega)}{2} + \sqrt{\frac{\eta_2^2(\omega)}{4} - 1}.$$

Construction of ICP

We obtain the Taylor series for the characteristic roots in a vicinity of $\omega = 0$

$$\lambda_{1,3}(\omega) = \frac{\eta_1(\omega)}{2} \mp \sqrt{\frac{\vartheta_1^2}{4} - 1} \cdot \cdot \sum_{n=0}^{\infty} \frac{(-1)^n\,(2n)!\,r_1^n(\omega)}{(1-2n)\,n!\,4^n\,(\theta_1+2)^n} \cdot \sum_{n=0}^{\infty} \frac{(-1)^n\,(2n)!\,r_1^n(\omega)}{(1-2n)\,n!\,4^n\,(\theta_1-2)^n}, \tag{11}$$

$$\lambda_{2,4}(\omega) = \frac{\eta_2(\omega)}{2} \mp \sqrt{\frac{\vartheta_2^2}{4} - 1} \cdot \cdot \sum_{n=0}^{\infty} \frac{(-1)^n\,(2n)!\,r_2^n(\omega)}{(1-2n)\,n!\,4^n\,(\theta_2+2)^n} \cdot \sum_{n=0}^{\infty} \frac{(-1)^n\,(2n)!\,r_2^n(\omega)}{(1-2n)\,n!\,4^n\,(\theta_2-2)^n}, \tag{12}$$

where $\eta_{1,2}$ are taken from (7), ϑ_j — from (9), $r_j(\omega) = \eta_j(\omega) - \vartheta_j$, $j = 1,\,2$.

Construction of ICP

The following inequalities are fulfilled as $\omega \to 0$

$$|\lambda_1|,\ |\lambda_2| < 1 < |\lambda_3|,\ |\lambda_4|.$$

Therefore, as $m \to +\infty$ it is possible to derive decreasing λ_1^m, λ_2^m and increasing λ_3^m, λ_4^m solutions of equation's (3) $\mathcal{Z}$-transformation. They form the fundamental set of solutions.

As with differential Eq. (2), for correctness of mixed initial-boundary value problem for finite-difference Eq. (3) two boundary conditions at each edge of the rod are required. We start by construction of $\mathcal{Z}$-image of the boundary conditions for the left edge in the form

$$P_1(\omega)\,v(0) + Q_1(\omega)\,v(h) + R_1(\omega)\,v(2h) + S_1(\omega)\,v(3h) = 0,$$
$$P_2(\omega)\,v(0) + Q_2(\omega)\,v(h) + R_2(\omega)\,v(2h) + S_2(\omega)\,v(3h) = 0,$$

where v is $\mathcal{Z}$-image of u. The equations correspond to

$$\sum_{j=0}^{\infty} p_{kj}\,u_0^{n-j} + \sum_{j=0}^{\infty} q_{kj}\,u_1^{n-j} + \sum_{j=0}^{\infty} r_{kj}\,u_2^{n-j} + \sum_{j=0}^{\infty} s_{kj}\,u_3^{n-j} = 0,\ k = 1,\,2, \tag{13}$$

where values p_{kj}, q_{kj}, q_{kj} and r_{kj} are the Taylor series coefficients before the term ω^j of the functions $P_k(\omega)$, $Q_k(\omega)$, $R_k(\omega)$, $S_k(\omega)$ correspondingly in a vicinity of the point $\omega = 0 \in \mathbb{C}$.

Building ICP and Hermite – Padé Approximation

Two linearly independent boundary conditions will provide ICP property, iff for the increasing Cauchy problem solutions $\nu(m) = \lambda_3^m$ and $\nu(m) = \lambda_4^m$ the symbols of the boundary conditions $\langle P_k, Q_k, R_k, S_k \rangle$, $(k = 1, 2)$ fulfil the following equations:

$$\begin{aligned} P_k + Q_k\,\lambda_3 + R_k\,\lambda_3^2 + S_k\,\lambda_3^3 = 0, \\ P_k + Q_k\,\lambda_4 + R_k\,\lambda_4^2 + S_k\,\lambda_4^3 = 0. \end{aligned} \qquad (14)$$

We relax the requirements to symbols of the operators of ICP boundary conditions, and exchange analytic functions in Syst. (14) by polynomials and exact equalities by asymptotic (as $\omega \to 0$) equalities:

$$\begin{cases} P_k(\omega) + Q_k(\omega)\,\lambda_3(\omega) + R_k(\omega)\,\lambda_3^2(\omega) + S_k(\omega)\,\lambda_3^3(\omega) = \mathbf{O}\left(\omega^{K_k}\right), \\ P_k(\omega) + Q_k(\omega)\,\lambda_4(\omega) + R_k(\omega)\,\lambda_4^2(\omega) + S_k(\omega)\,\lambda_4^3(\omega) = \mathbf{O}\left(\omega^{K_k}\right). \end{cases} \qquad (15)$$

If we choose normalisation condition at $k = 1$:

$$P_1(0) = p_{1,0} = 1,\ Q_1(0) = q_{1,0} = 0,$$

we are able to compute the boundary value on the n-th temporal step u_0^n. We obtain the first boundary condition in the form:

$$u_0^n + \sum_{j=1}^{\mathbf{deg}\,P_1} p_{1j}\, u_0^{n-j} + \sum_{j=1}^{\mathbf{deg}\,Q_1} q_{1j}\, u_1^{n-j} + \sum_{j=0}^{\mathbf{deg}\,R_1} r_{1j}\, u_2^{n-j} + \sum_{j=0}^{\mathbf{deg}\,S_1} s_{1j}\, u_3^{n-j} = 0. \tag{16}$$

Similarly we choose normalisation condition at $k = 2$:

$$P_2(0) = p_{2,0} = 0,\ Q_2(0) = q_{2,0} = 1,$$

to obtain the preboundary value:

$$u_1^n + \sum_{j=1}^{\mathbf{deg}\,P_2} p_{2j}\, u_0^{n-j} + \sum_{j=1}^{\mathbf{deg}\,Q_2} q_{2j}\, u_1^{n-j} + \sum_{j=0}^{\mathbf{deg}\,R_2} r_{2j}\, u_2^{n-j} + \sum_{j=0}^{\mathbf{deg}\,S_2} s_{2j}\, u_3^{n-j} = 0.$$

Parameters and Initial Conditions

For our experiments we choose rod's parameters (that are similar to steel) and steps:

ρ	$= 7860\,\mathrm{kg\,m^{-3}}$	L	$= 1\,\mathrm{m}$
E	$= 210 \cdot 10^9\,\mathrm{Pa}$	T	$= 0.04\,\mathrm{s}$
R	$= 10^{-3}\,\mathrm{m}$	ν	≈ 4.2748
h	$= 0.02\mathrm{m}$	μ	$= 0.0025$
τ	$= 1.6 \cdot 10^{-4}\,\mathrm{s}$		

Table 1: Parameters of our numerical experiments

We set initial conditions for Eq. (2) as $u(0,x) = x\exp\left(-\frac{x^2}{0.02}\right)$ and $\frac{\partial u}{\partial t}(0,x) = 0$ for $x \in [-L/2,\ L/2]$.

Parameters and Initial Conditions

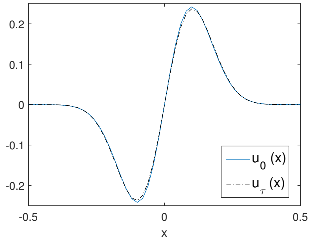

(a)

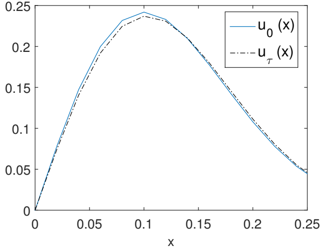

(b)

Figure 1: Initial functions $u_0(x),\ u_1(x)$ for two first time steps: (a) — for the segment $x \in [-L/2,\ L/2]$; (b) — in the vicinity of their maximal value.

Parameters and Initial Conditions

We define a reference solution $u^*(t, x)$ on the extended segment $[-15L, 15L]$, see Fig. 2.

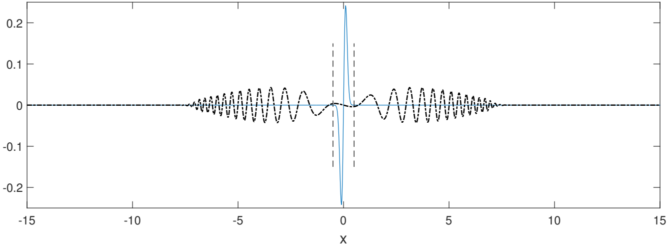

Figure 2: Reference solution u^* on the extended segment $[-15\,L, 15\,L]$. Solid line — solution at the initial time moment $t = 0$, dash-dotted line – in the final time moment $t = T$. Two vertical dashed lines indicate the borders of considered segment $x \in [-L/2, L/2]$. The boundary conditions do not influence the reference solution u^* during the integration time T

Basic Version of the ICP Boundary Conditions

Let us consider a set of polynomial degrees

$$\deg P_k = \deg Q_k = 4,\ \deg R_k = \deg S_k = 8, \quad k = 1,\, 2. \qquad (18)$$

Here and below we consider equal sets of polynomial degrees for border and preborder boundary conditions.
To evaluate the dynamics of error of Eq. (3) solution u under ICP boundary conditions, we use common logarithm of the Chebyshev norm $\mathbf{C}[-L/2,\, L/2]$ of solutions' difference, i.e.

$$\lg \max_{j=0,1,\dots,N} |u(t, x_j) - u^*(t, x_j)|\,.$$

Results of numeric experiment with ICP boundary sets $\langle 4,\, 4,\, 8,\, 8 \rangle$ are presented in Fig. 3.

Modification of the ICP Boundary Conditions

The function $u(t, x) \equiv \text{const}$ is a solution of differential Eq. (2) and the finite-difference Eq. (3). We can additionally require the ICP boundary conditions to satisfy this solution. In other words, we introduce an additional linear condition on the polynomial coefficients – their sums are equal to zero:

$$P_k(1) + Q_k(1) + R_k(1) + S_k(1) = 0, \quad k = 1, 2. \tag{19}$$

To keep the same order of approximation, let us consider polynomial's degrees

$$\deg P_k = 4, \ \deg Q_k = 5, \ \deg R_k = \deg S_k = 8, \quad k = 1, 2. \tag{20}$$

Modification Impact

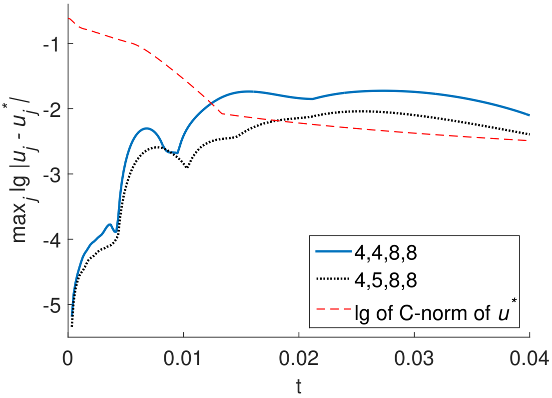

Figure 3: Common logarithm of **C**-norm of the difference between reference solution u^* and solutions with ICP boundary conditions

ICP Boundary Conditions' Comparison

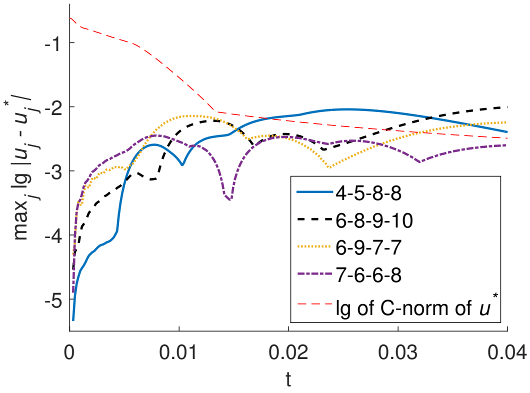

Figure 4: Logarithm of **C**-norm of the difference between reference solution u^* and solutions with ICP boundary conditions under additional requirement Eq. (19)

"Usual" Homogeneous Boundary Conditions

In practice simple homogeneous boundary conditions (i.e., Dirichlet, Neumann) lead to partial or complete reflection of outgoing waves back into calculation area (sometimes with increased amplitude). Consider some "usual" homogeneous boundary conditions:

i) $u|_\Gamma = 0,\ \frac{\partial u}{\partial x}\Big|_\Gamma = 0 \implies u_0^n = u_1^n = 0,$

ii) $u|_\Gamma = 0,\ \frac{\partial^2 u}{\partial x^2}\Big|_\Gamma = 0 \implies u_0^n = 0,\ u_1^n = u_2^n/2,$

iii) $\frac{\partial^2 u}{\partial x^2}\Big|_\Gamma = 0,\ \frac{\partial^3 u}{\partial x^3}\Big|_\Gamma = 0 \implies u_0^n = 3u_2^n - 2u_3^n,\ u_1^n = 2u_2^n - u_3^n,$

iv) ICP boundary condition with polynomials degrees Eq. (20) under additional requirement Eq. (19).

Fig. 5 shows the dynamics of solutions errors that are calculated using various boundary conditions:

"Usual" Homogeneous Boundary Conditions

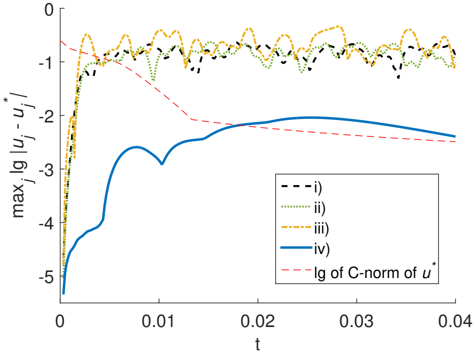

Figure 5: Dashed, dotted and dash-dotted lines — logarithm of **C**-norm of the difference between reference solution u^* and solution with "usual" boundary conditions. Solid line corresponds to the ICP boundary conditions with additional requirement Eq. (19)

Conclusions

1. The ICP boundary conditions were constructed for the finite-difference Crank – Nicolson implicit approximation of the transverse vibrations equation of a rod with a circular cross section.
2. Differential and finite-difference equations require two boundary conditions on each end.
3. Special vectorial version of the rational Hermite – Padé approximation provides economical and exact realisations of the ICP boundary conditions.
4. Shown that "usual" homogeneous boundary conditions do not have "transparency" property.
5. ICP boundary conditions can be calculated for different model's parameters.
6. ICP boundary conditions with additional relation: exactness on the constants is preferable.